GEOPHYSICAL RESEARCH LETTERS, VOL. 27, NO. 11, PAGES 1639-1642, JUNE 1, 2000

Detection of a lightning influence on tropical tropospheric ozone

Randall V. Martin, Daniel J. Jacob, and Jennifer A. Logan

Division of Engineering and Applied Sciences and Department of Earth and Planetary Sciences, Harvard University, Cambridge, Massachusetts

Jerry M. Ziemke[1]

Software Corporation of America, Beltsville, Maryland

Richard Washington

School of Geography, Oxford University, Oxford, United Kingdom

Abstract. Empirical orthogonal functions (EOFs) are used to analyze a 14-year record of tropical tropospheric ozone columns (TTOCs) determined from satellite measurements. The first EOF explains 54% of TTOC variance and represents biomass burning in Africa and South America. The second EOF explains 20% of the variance and has a distinct lightning signature.

Introduction

Ozone (O_3) in the tropical troposphere plays a key role in determining the oxidizing power of the atmosphere and is an important greenhouse gas. Production of O_3 in the tropical troposphere is believed to be controlled by the supply of nitrogen oxide radicals ($NO_x \equiv NO + NO_2$) originating from lightning, biomass burning, and soils [*Jacob et al.*, 1996]. Global model calculations suggest that most of the NO_x in the tropical troposphere is from lightning [*Lamarque et al.*, 1996], but to date there are no clear observations of large-scale O_3 enhancements associated with emissions of NO_x from lightning. This is in contrast to the large springtime enhancements of O_3 in the southern tropics caused by NO_x emissions from biomass burning [*Thompson et al.*, 1996; *Schultz et al.*, 1999].

Part of the problem in detecting a lightning influence on O_3 may be that most of the lightning NO_x is released in the upper troposphere where O_3 production is slow even though the number of O_3 molecules produced per unit NO_x consumed is high. If so, the advent of global observation capability from satellites should greatly facilitate detection.

We present here evidence of a large-scale lightning influence on tropical tropospheric O_3 using a 14-year record of monthly tropical tropospheric ozone columns (TTOCs) determined by *Ziemke et al.* [1998] from the Total Ozone Mapping Spectrometer (TOMS) aboard the Nimbus 7 satellite. We show that empirical orthogonal functions (EOFs) of TTOCs relate significantly to lightning NO_x emissions. EOFs represent an orthogonal basis upon which the monthly spatial fields of TTOCs can be decomposed, offering an objective analysis of the spatial and temporal patterns of variability.

Data and Methods

We used monthly-mean TTOCs over the period 1979–1992 (inclusive) derived by *Ziemke et al.* [1998] from Nimbus 7 TOMS observations using the convective cloud differential method. The central assumption of this method is that cloud tops over the equatorial Pacific usually extend to the tropopause. Since longitudinal variability in stratospheric column O_3 is small in the tropics, stratospheric O_3 columns can be derived by averaging above-cloud column O_3 amounts over the equatorial Pacific. The resulting monthly TTOCs are reported by *Ziemke et al.* [1998] on a $5^\circ \times 5^\circ$ grid between 15S and 15N (Figure 1).

Because the convective cloud differential method does not rely upon other satellite O_3 measurements, its error is reduced over that of TOMS-SAGE [*Fishman and Brackett*, 1997] or TOMS-SBUV [*Fishman et al.*, 1996]. An alternate retrieval of TTOCs from TOMS observations has been reported by *Hudson and Thompson* [1998], but provides a continuous record from only 9S to 7N during 1979–92.

Our analysis compares the TTOCs from *Ziemke et al.* [1998] to global lightning NO_x emission estimates available from *Price et al.* [1997] on a $2.5^\circ \times 2.5^\circ$ grid with monthly resolution. The latter estimates parameterize lightning frequencies and intensities as a function of cloud top data at 5 km resolution in 1983–91 from the International Satellite Cloud Climatology Project (ISCCP) [*Rossow and Schiffer*, 1991].

Figure 2 illustrates the seasonal variation in tropical lightning NO_x as derived by *Price et al.* [1997]. Lightning occurs mainly over continents since the relatively weak updrafts in marine storms result in considerably fewer electrical discharges. Lightning NO_x emissions vary with seasonal solar heating and are highest during DJF (JJA) in the southern (northern) tropics. We find that 28% of lightning NO_x in the 15S to 15N latitudinal band is produced over Africa, 34% over South America, and 38% over southeast Asia and Oceania.

We averaged the monthly TTOCs from *Ziemke et al.* [1998] over the 14-year period (1979–92) to yield one year of

[1]Also at NASA Goddard Space Flight Center, Maryland.

Paper number 1999GL011181.
0094-8276/00/1999GL011181$05.00

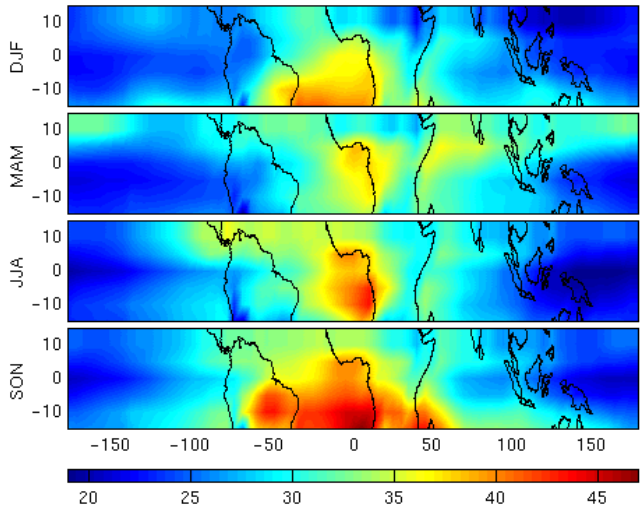

Figure 1. Seasonally averaged tropical tropospheric ozone columns (TTOCs) in Dobson Units (DU) from Nimbus 7 TOMS for 1979–92. Data from *Ziemke et al.* [1998].

monthly means that are representative of TTOC seasonal variation. The EOFs were calculated from the monthly mean TTOCs, $\mathbf{T}$, after weighting them by $\sqrt{\cos}$ of the latitude to adjust for the poleward decreasing area of each grid box [*Chung and Nigam*, 1999], a minor adjustment for the tropics. The spatial loading patterns or EOFs are the eigenvectors, $\mathbf{e}^{(i)}$, of the temporal covariance matrix of TTOCs. The i-th eigenvalue defines the fraction of TTOC variance accounted for by $\mathbf{e}^{(i)}$. The corresponding seasonal variation $\mathbf{s}^{(i)}$, commonly referred to as the principal component, is the product of $\mathbf{e}^{(i)}$ and the weighted monthly mean TTOCs with their annual mean, $\bar{\mathbf{T}}$, removed

$$\mathbf{s}^{(i)} = (\mathbf{T} - \bar{\mathbf{T}})\mathbf{e}^{(i)}. \quad (1)$$

With this definition, $\mathbf{s}^{(i)}$ is the i-th vector of 12 components (one for each month) which describes the seasonal variation in the i-th EOF. The original monthly mean TTOCs for a given month (m) can then be expressed as a function of the annual mean, the ensemble of EOFs, and the corresponding monthly component of $\mathbf{s}^{(i)}$

$$\mathbf{T}(m) = \mathbf{T} + \sum_i \mathbf{s}^{(i)}(m)\mathbf{e}^{(i)}. \quad (2)$$

We find that Varimax rotated EOFs [e.g., *Kim and Wu*, 1999] have similar spatial loading patterns and seasonal variation as the unrotated EOFs presented here.

Results

The three leading EOFs Figure 3 together explain almost 90% of the seasonal TTOC variability. The 4th EOF (not shown) represents less than 6%. Figure 3a shows the spatial loading pattern of each EOF, with corresponding seasonal variation in Figure 3b. Our analysis does not account for interannual variability of TTOCs which *Ziemke and Chandra* [1999] found to be driven primarily by the El Niño-Southern Oscillation in the Pacific and secondarily by the quasi-biennial oscillation in the Atlantic. Independent calculations of EOFs that included and excluded El Niño years showed little difference relative to the results in Figure 3.

The first EOF (EOF1) captures 54% of TTOC variability with an unequivocal biomass burning signature that peaks in September and October over Brazil and the southern tropical Atlantic. Ozone concentrations in the southern tropics reach their seasonal maxima in September and October [*Olson et al.*, 1996] due to widespread biomass burning in Brazil and southern Africa [*Thompson et al.*, 1996]. Ozone production in that time of year is thought to be enhanced by proximal deep convective systems in southern Africa [*Jenkins et al.*, 1997]. Biomass burning decreases with the onset of the wet season in concurrence with TTOCs in the positive region of EOF1.

The second EOF (EOF2) explains 20% of TTOC variability and is seasonally in phase with lightning, peaking in the north (south) during the boreal (austral) summer. The prominent features of a maximum in Oceania during DJF and a maximum in Central America during JJA replicate similar features in the lightning NO_x source distribution (Figure 2). We projected the spatial distribution of EOF2 (Figure 3a) upon the monthly gridded lightning NO_x emissions of *Price et al.* [1997] by calculating their product (Eq. 1). The monthly variation of this lightning projection correlates significantly with the seasonal variation of EOF2 ($r = 0.88$, $p < 0.0005$, $n = 12$) supporting our attribution of EOF2 to a lightning source of O_3.

We examined the EOFs of the lightning NO_x emissions of *Price et al.* [1997] to provide an alternate perspective. The first EOF (Figure 4) accounts for 76% of the variance. It features a broad maximum during DJF (JJA) in the south (north) and correlates significantly with EOF2 ($r = 0.89$, $p < 0.0005$, $n = 12$). The results from extended EOFs [e.g., *Kim and Wu*, 1999] of both lightning and O_3 also support the relationship between EOF2 and lightning NO_x emissions. The third EOF (EOF3) explains 15% of the TTOC variance with a maximum in March-April and a secondary maximum in October. The March-April maximum appears to reflect the Southeast Asian biomass burning season [*Liu et al.*, 1999] and meridional transport from the northern extratropics where O_3 is at its seasonal peak. The physical meaning of the October secondary maximum is unclear.

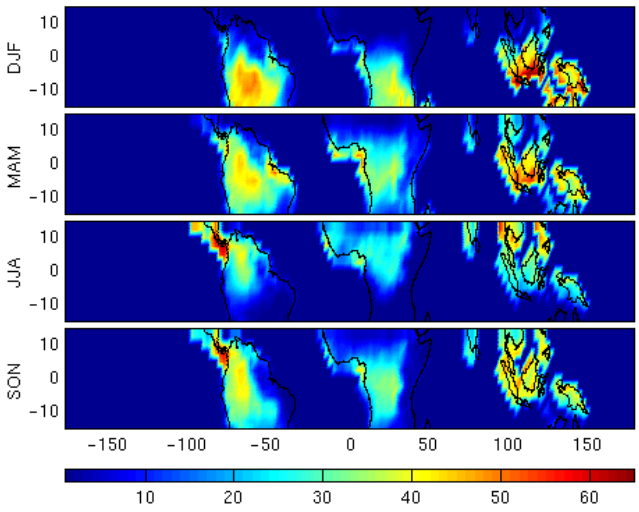

Figure 2. Seasonally averaged lightning NO_x emissions in units of 10^9 atoms nitrogen (N) $cm^{-2}s^{-1}$. Data from *Price et al.* [1997].

Discussion

Other known factors of tropical O_3 variability do not correlate with EOF2. The Walker Circulation over the equatorial Pacific is most active in DJF [*Webster and Yang*, 1992] with associated rapid convective overturning that enhances destruction of O_3 in the tropospheric column [*Lelieveld and Crutzen*, 1994]. EOF2 has the opposite seasonal pattern. Emission of NO_x from tropical soils peaks in the dry season [*Bakwin et al.*, 1990], again inconsistent with EOF2.

EOF2 is slightly distorted by the biomass burning season south of the Congo Basin that peaks in June and July [*Justice et al.*, 1996]. Figure 1 illustrates the tropical Atlantic O_3 enhancement concurrent with the June-July biomass burning season south of the Congo Basin. This small biomass burning signal appears in EOF2 due to its temporal correlation with the seasonal variation in lightning NO_x.

EOFs calculated separately for the continental regions of South America, Africa, and Indonesia (not shown) provide further support to the hypothesis of lightning NO_x influencing the distribution of TTOCs. Because each continent has slightly different biomass burning seasons, performing the calculation separately on each continent allows EOF1 to more accurately represent biomass burning. As a result, in each case EOF2 more clearly represents the latitudinal variation associated with the seasonal movement of lightning activity. The TTOC variances explained by EOF2 for South America and Indonesia increase to 24% and 34%, respectively. In Africa where lightning NO_x is weaker and the biomass burning season more intense, the variance explained by EOF2 decreases to 17%.

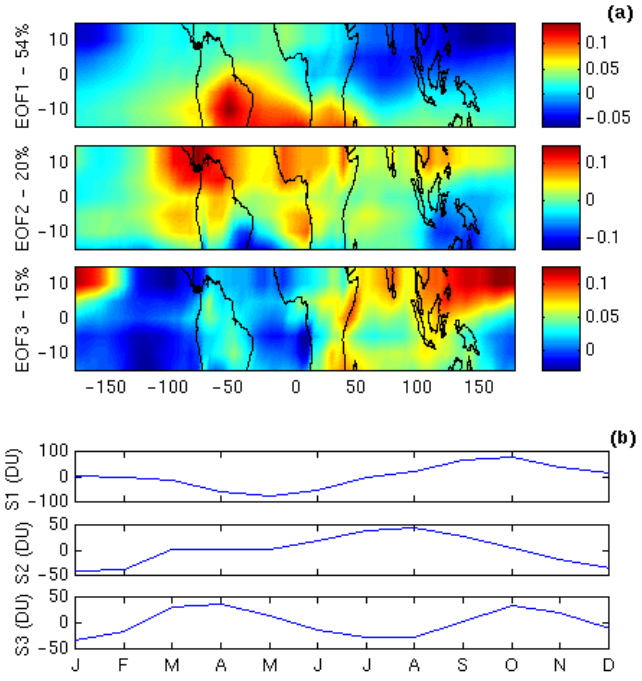

Figure 3. (a) Spatial loading patterns, $\mathbf{e}^{(i)}$, of the first three EOFs of TTOCs. The colorbar units are dimensionless. (b) Corresponding seasonal variations, $\mathbf{s}^{(i)}$ (DU), of each EOF when projected upon the data in Figure 1 (Eq. 1). EOF1 accounts for 54% of the seasonal variance of TTOCs, EOF2 for 20% and EOF3 for 15%.

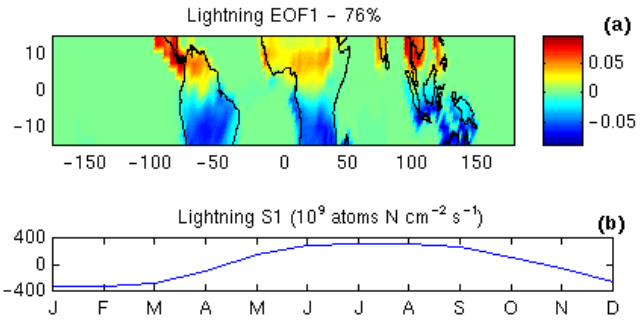

Figure 4. Spatial loading pattern, $\mathbf{e}^{(1)}$, of the first EOF of lightning NO_x accounting for 76% of the variance. The colorbar units are dimensionless. (b) Corresponding seasonal variation when projected upon the data in Figure 2 (Eq. 1).

Remarkably, the TTOCs from TOMS show no O_3 enhancement over northern (sub-Saharan) Africa during the biomass burning season between December and March. In situ observations in that region show that high aerosol and O_3 concentrations from biomass burning are largely confined to the lower troposphere by a strong inversion [*Marenco et al.*, 1990; *Andreae et al.*, 1992]. The collocation of aerosols with high O_3 in the northern tropics would reduce the sensitivity of TOMS to O_3 from biomass burning. In contrast, during the Southern Hemisphere biomass burning season, O_3 is enhanced in the middle and upper troposphere where it is not associated with aerosols because of scavenging [*Browell et al.*, 1996]. Although a correction for aerosols has been included in the TOMS retrieval algorithm [*Torres and Bhartia*, 1999], it may not be sufficient. Furthermore, the TOMS retrieval algorithm is generally insensitive to O_3 variability in the lower troposphere due to Rayleigh scattering and the assumption of a standard O_3 profile [*McPeters et al.*, 1996]. These uncertainties probably affect regions other than northern Africa. The EOFs presented here are therefore more indicative of middle and upper tropospheric variability than of lower tropospheric variability.

The EOF analysis is a linear decomposition but the dependence of O_3 on NO_x is nonlinear. Although the 20% contribution of EOF2 to the O_3 variance does imply a significant effect of lightning on tropical tropospheric O_3, it does not mean that lightning accounts for 20% of the O_3 variance. Quantitative interpretation of the EOF information in terms of the O_3 budget must be done within the framework of a global three-dimensional model. Reproducing the observed EOFs represent a critical test of the ability of a model to capture the dominant patterns of O_3 variability.

Acknowledgments. This work was supported by the National Aeronautics and Space Administration and by a National Science Foundation fellowship for Randall Martin. We gratefully thank Colin Price for providing the lightning NO_x emissions used in this study.

References

Andreae, M. O., et al., Ozone and aitken nucei over equatorial Africa: Airborne observations during DECAFE 88, *J. Geophys. Res., 97*, 6137–6148, 1992.

Bakwin, P. S., S. C. Wofsy, S.-M. Fan, M. Keller, S. E. Trumbore, and J. M. da Costa, Emission of nitric oxide (NO) from tropical forest soils and exchange of NO between the forest canopy and

atmospheric boundary layers, *J. Geophys. Res., 95*, 16755–16764, 1990.

Browell, E. V., et al., Ozone and aerosol distributions and air mass characteristics over the South Atlantic Basin during the burning season, *J. Geophys. Res., 101*, 24043–24068, 1996.

Chung, C., and S. Nigam, Weighting of geophysical data in Principal Component Analysis, *J. Geophys. Res., 104*, 16925–16928, 1999.

Fishman, J., and V. G. Brackett, The climatological distribution of tropospheric ozone derived from satellite measurements using version 7 Total Ozone Mapping Spectrometer and Stratospheric Aerosol and Gas Experiment data sets, *J. Geophys. Res., 102*, 19275–19278, 1997.

Fishman, J., V. G. Brackett, E. V. Browell, and W. B. Grant, Tropospheric ozone derived from TOMS/SBUV measurements during TRACE A, *J. Geophys. Res., 101*, 24069–24082, 1996.

Hudson, R. D., and A. M. Thompson, Tropical tropospheric ozone from total ozone mapping spectrometer by a modified residual method, *J. Geophys. Res., 103*, 22129–22145, 1998.

Jacob, D. J., et al., Origin of ozone and NO_x in the tropical troposphere: A photochemical analysis of aircraft observations over the South Atlantic basin, *J. Geophys. Res., 101*, 24235–24250, 1996.

Jenkins, G. S., K. Mohr, V. R. Morris, and O. Arino, The role of convective processes over the Zaire-Congo Basin to the Southern Hemispheric ozone maximum, *J. Geophys. Res., 102*, 18963–18980, 1997.

Justice, C. O., J. D. Kendall, P. R. Dowty, and R. J. Scholes, Satellite remote sensing of fires during the SAFARI campaign using NOAA advanced very high resolution radiometer data, *J. Geophys. Res., 101*, 23851–23863, 1996.

Kim, K.-Y., and Q. Wu, A comparison study of EOF techniques: Analysis of nonstationary data with periodic statistics, *J. Climate*, *12*, 185-199, 1999.

Lamarque, J.-F., G. P. Brasseur, P. G. Hess, and J.-F. Müller, Three-dimensional study of the relative contributions of the different nitrogen sources in the troposphere, *J. Geophys. Res., 101*, 22955–22968, 1996.

Lelieveld, J., and P. J. Crutzen, Role of deep cloud convection in the ozone budget of the troposphere, *Science*, *264*, 1759–1761, 1994.

Liu, H., W. L. Chang, S. J. Oltmans, L. Y. Chan, and J. M. Harris, On springtime high ozone events in the lower troposphere from Southeast Asian biomass burning, *Atmos. Environ.*, *33*, 2403–2410, 1999.

Marenco, A., J. C. Medale, and S. Prieur, Study of tropospheric ozone in the tropical belt (Africa, America) from STRATOZ and TROPOZ campaigns, *Atmos. Environ.*, *24A*, 2823–2834, 1990.

McPeters, R. D., et al., Nimbus-7 Total ozone Mapping Spectrometer (TOMS) Data Products User's Guide, pp. 67, 1996.

Olson, J. R., J. Fishman, V. W. J. H. Kirchhoff, D. Nganga, and B. Cros, Analysis of the distribution of ozone over the southern Atlantic, *J. Geophys. Res., 101*, 24083–24093, 1996.

Price, C., J. Penner, and M. Prather, NO_x from lightning 1. Global distribution based on lightning physics, *J. Geophys. Res., 102*, 5929–5941, 1997.

Rossow, W. B., and R. A. Schiffer, ISCCP cloud data products, *Bull. Am. Meteorol. Soc.*, *72*, 2–20, 1991.

Schultz, M., et al., On the origin of tropospheric ozone and NO_x over the tropical Pacific, *J. Geophys. Res., 104*, 5829–5844, 1999.

Thompson, A. M., et al., Where did tropospheric ozone over southern Africa and the tropical Atlantic come from in October 1992 — insights from TOMS, GTE TRACE A, and SAFARI 1992, *J. Geophys. Res., 101*, 24251–24278, 1996.

Torres, O., and P. K. Bhartia, Impact of tropospheric aerosol absorption on ozone retrieval from backscattered ultraviolet measurements, *J. Geophys. Res., 104*, 21569–21577, 1999.

Webster, P. J., and S. Yang, Monsoon and ENSO: Selectively interactive systems, *Q. J. R. Meteorol. Soc., 118*, 877–926, 1992.

Ziemke, J. R., and S. Chandra, Seasonal and interannual variabilities in tropical tropospheric ozone, *J. Geophys. Res., 104*, 21425–21442, 1999.

Ziemke, J. R., S. Chandra, and P. K. Bhartia, Two new methods for deriving tropospheric column ozone from TOMS measurements; Assimilated UARS MLS/HALOE and convective-cloud differential techniques, *J. Geophys. Res., 103*, 22115–22127, 1998.

D. J. Jacob, J. A. Logan, and R. V. Martin, 29 Oxford Street, Cambridge, MA 02138 (e-mail: djj, jal, or rvm@io.harvard.edu)

R. Washington, School of Geography, Oxford OX1 3JA, United Kingdom (e-mail: richard.washington@geography.ox.ac.uk)

J. R. Ziemke, Software Corporation of America, Beltsville, MD 20705 (e-mail: ziemke@chescat.gsfc.nasa.gov)

(Received October 27, 1999; revised March 7, 2000; accepted March 16, 2000.)